

Scanning plasmonic microscopy by image reconstruction from the Fourier space

Oriane Mollet, Serge Huant, and Aurélien Drezet

Institut Néel, CNRS and Université Joseph Fourier, BP166, 38042 Grenoble Cedex, France

aurelien.drezet@grenoble.cnrs.fr

Abstract: We demonstrate a simple scheme for high-resolution imaging of nanoplasmonic structures that basically removes most of the resolution limiting allowed light usually transmitted to the far field. This is achieved by implementing a Fourier lens in a near-field scanning optical microscope (NSOM) operating in the leakage-radiation microscopy (LRM) mode. The method consists of reconstructing optical images solely from the plasmonic ‘forbidden’ light collected in the Fourier space. It is demonstrated by using a point-like nanodiamond-based tip that illuminates a thin gold film patterned with a sub-wavelength annular slit. The reconstructed image of the slit shows a spatial resolution enhanced by a factor $\simeq 4$ compared to NSOM images acquired directly in the real space.

© 2018 Optical Society of America

OCIS codes: (240.6680) Surface plasmons; (180.4243) Near-field microscopy; (180.5810) Scanning microscopy; (050.6624) Subwavelength structures

References and links

1. B. Hecht, D. W. Pohl, H. Heinzelmann, and L. Novotny, “Tunnel near-field optical microscopy: TNOM-2,” *Ultramicroscopy* **61**, 99-104 (1995).
2. B. Hecht, H. Bielefeldt, L. Novotny, Y. Inouye, and D. W. Pohl, “Local excitation, scattering, and interference of surface plasmons,” *Phys. Rev. Lett.* **77**, 1889-1892 (1996).
3. C. Chicane, T. David, R. Quidant, J.-C. Weeber, Y. Lacroute, E. Bourillot, A. Dereux, G. Colas Des Francs, and C. Girard, “Imaging the Local Density of States of Optical Corrals,” *Phys. Rev. Lett.* **88**, 097402 (2002).
4. A. Bouhelier, Th. Huser, H. Tamaru, H.-J. Güntherodt, and D. W. Pohl, “Plasmon optics of structured silver films,” *Phys. Rev. B* **63**, 155404 (2001).
5. A. Drezet, A. Hohenau, A. L. Stepanov, H. Ditlbacher, B. Steinberger, N. Galler, F. R. Aussenegg, A. Leitner, and J. R. Krenn, “How to erase surface plasmon fringes,” *Appl. Phys. Lett.* **89**, 091117 (2006).
6. D. E. Chang, A. S. Sørensen, P. R. Hemmer, and M. D. Lukin, “Quantum Optics with Surface Plasmons,” *Phys. Rev. Lett.* **97**, 053002 (2006).
7. A. V. Akimov, A. Mukherjee, C. L. Yu, D. E. Chang, A. S. Zibrov, P. R. Hemmer, H. Park, and M. D. Lukin, “Generation of single optical plasmons in metallic nanowires coupled to quantum dots,” *Nature* **450**, 402-406 (2007).
8. S. Schietinger, M. Barth, T. Aichele, and O. Benson, “Plasmon-enhanced single photon emission from a nanoassembled metal-diamond hybrid structure at room temperature,” *Nano Lett.* **9**, 1694-1698 (2009).
9. Y. Fedutik, V.V. Temnov, O. Schöps, U. Woggon, and M.V. Artemyev, “Exciton-Plasmon-Photon Conversion in Plasmonic Nanostructures,” *Phys. Rev. Lett.* **99**, 136802 (2007).
10. A. W. Schell, G. Kewes, T. Hanke, A. Leitenstorfer, R. Bratschitsch, O. Benson, and T. Aichele, “Single defect centers in diamond nanocrystals as quantum probes for plasmonic nanostructures,” *Opt. Express* **19**, 7914-7920 (2011).
11. R. Kolesov, B. Grotz, G. Balasubramanian, R. J. Stöhr, A. A. L. Nicolet, P. R. Hemmer, F. Jelezko, and J. Wrachtrup, “Wave-particle duality of single surface plasmon polaritons,” *Nature Phys.* **5**, 470-474 (2009).
12. A. Huck, S. Kumar, A. Shakoov, and U. Andersen, “Controlled Coupling of a Single Nitrogen-Vacancy Center to a Silver Nanowire,” *Phys. Rev. Lett.* **106**, 096801 (2011).

13. A. Cuche, A. Drezet, Y. Sonnefraud, O. Faklaris, F. Treussart, J.-F. Roch, and S. Huant, "Near-field optical microscopy with a nanodiamond-based single-photon tip," *Opt. Express* **17**, 19969-19980 (2009).
14. A. Drezet, A. Cuche, and S. Huant, "Near-field microscopy with a single-photon point-like emitter: Resolution versus the aperture tip?," *Opt. Commun.* **284**, 1444-1450 (2011).
15. Y. Sonnefraud, A. Cuche, O. Faklaris, J.-P. Boudou, T. Sauvage, J.-F. Roch, F. Treussart, and S. Huant, "Diamond nanocrystals hosting single nitrogen-vacancy color centers sorted by photon-correlation near-field microscopy," *Opt. Lett.* **33**, 611-613 (2008).
16. A. Cuche, O. Mollet, A. Drezet, and S. Huant, "'Deterministic' quantum plasmonics," *Nano Lett.* **10**, 4566-4570 (2010).
17. O. Mollet, A. Cuche, A. Drezet, and S. Huant, "Leakage radiation microscopy of surface plasmons launched by a nanodiamond-based tip," *Diam. Relat. Mater.* **20**, 995-998 (2011).
18. O. Mollet, S. Huant, G. Dantelle, T. Gacoin, and A. Drezet, "Quantum plasmonics: Second-order coherence of surface plasmons launched by quantum emitters into a metallic film," *Phys. Rev. B* **86**, 045401 (2012).
19. S. Kühn, C. Hettich, C. Schmitt, J.-P. Poizat, and V. Sandoghdar, "Diamond colour centres as a nanoscopic light source for scanning near-field optical microscopy," *J. Microsc.* **202**, 2-6 (2001).
20. R. Marty, C. Girard, A. Arbouet, and G. Colas des Francs, "Near-field coupling of a Point-like dipolar source with a thin metallic film: Implication for STM plasmon excitations," *Chem. Phys. Lett.* **532**, 100-105 (2012).
21. A. Gruber, A. Drabenstedt, C. Tietz, L. Fleury, J. Wrachtrup, and C. von Borczyskowski, "Scanning confocal optical microscopy and magnetic resonance on single defect centers," *Science* **276**, 2012-2014 (1997).
22. K. Karrai and R. D. Grober, "Piezoelectric tip-sample distance control for near field optical microscopes," *Appl. Phys. Lett.* **60**, 1842-1844 (1995).
23. Slight dispersions in the measured rim width are due to an imperfect patterning during the FIB milling process.
24. C. Girard, O. J. F. Martin, G. Leveque, G. Colas des Francs, A. Dereux, "Generalized bloch equations for optical interactions in confined geometries," *Chem. Phys. Lett.* **404**, 44-48 (2005).
25. R. Marty, A. Arbouet, V. Paillard, C. Girard, and G. Colas des Francs, "Photon antibunching in the optical near-field," *Phys. Rev. B* **82**, 081403 (2010).
26. F. I. Baida, D. Van Labeke, A. Bouhelier, T. Huser, D. Pohl, "Propagation and diffraction of locally excited surface plasmons," *J. Opt. Soc. Am. A* **18**, 1552-1561 (2001).
27. L. Novotny, B. Hecht and D. Pohl, "Interference of locally excited surface plasmons," *J. Appl. Phys.* **81**, 1798-1806 (1997).
28. A. Hohenau, J. R. Krenn, A. Drezet, O. Mollet, S. Huant, C. Genet, B. Stein, and T. W. Ebbesen, "Surface plasmon leakage radiation microscopy at the diffraction limit," *Opt. Express* **19**, 25749-25762 (2011).
29. M. Specht, J. D. Pedarnig, W. M. Heckl, and T. W. Hänsch, "Scanning plasmon near-field microscope," *Phys. Rev. Lett.* **68**, 476-479 (1992).
30. T. Wang, E. Boer-Duchemin, Y. Zhang, G. Comtet, and G. Dujardin, "Excitation of propagating surface plasmons with a scanning tunneling microscope," *Nanotechnology* **22**, 175201 (2011).
31. P. Bharadwaj, A. Bouhelier, and L. Novotny, "Electrical excitation of surface plasmons," *Phys. Rev. Lett.* **106**, 226802 (2011).

1. Introduction

A sub-wavelength object diffracts light into evanescent and propagating waves. It is the evanescent part - the so-called forbidden light - that carries information on the sub-wavelength details of the object. This evanescent contribution plays a key role in experiments targeted at imaging surface-plasmon polaritons (SPPs), which are electron-photon hybrid states naturally confined at the boundary between a metal and an insulator. As such, SPPs are strongly modified by local changes of their environment at the nanoscale and it is therefore critical to find efficient methods to probe the interaction of SPPs with nanostructures. This constitutes the central motivation of the present work. In this context, imaging SPPs can be achieved using the 'forbidden light' NSOM arrangement [1-4], where the forbidden light that couples into the sample glass substrate at angles larger than the critical incidence ($\theta_C \simeq 43.2^\circ$ in fused silica of optical index $n \simeq 1.46$) is collected by an elliptic mirror. An alternative method to collect the plasmonic forbidden light uses a Fourier lens placed in the optical path of a LRM setup to selectively image in the Fourier space SPP beams propagating along specific directions [5].

In this paper, we consider a sub-wavelength slit patterned in a thin gold film that we image with a NSOM using a point-like optical tip for illumination. Our first motivation is to extend previous works [1-5] by demonstrating that the use of Fourier space SPP signals for image re-

construction of this nanostructure provides optical images that are much better resolved (about 4 times) compared to images acquired in the real space directly. Our second motivation is related to the emerging field of quantum plasmonics, where one or several quantum emitters are coupled to plasmonic nanostructures to generate single SPP quanta [6-12]. This field is usually dealing with weak optical signals that can be polluted by a range of spurious incoherent light originating, e.g., from gold fluorescence. Cleaning the useful quantum-related information from spurious incoherent signals could be crucial for future quantum plasmonics experiments: in addition to offering enhanced spatial resolution, our method offers a powerful way of making this cleaning step. This is demonstrated here by using as point-like optical tip a scanning quantum source of light made of a single fluorescent nanodiamond glued at the apex of a fiber tip [13-18].

2. Experiment

A sketch of our setup is shown in Fig. 1. Basically, this is a transmission NSOM making use of a fluorescent nanodiamond-based optical tip [13, 19] for illumination of a thin (30 nm) gold film deposited on a fused silica cover slip. Our motivations for using such a tip are multiple. First, the small size (≈ 25 nm) of the nanodiamond mimics a point-like source of light, which has the potential for a better spatial resolution than standard metal-coated optical tips [14] (ultimately limited only by the scan height of the point source over the structure). This nanodiamond hosts three to four Nitrogen-Vacancy (NV) color-centers as revealed by time-intensity second-order

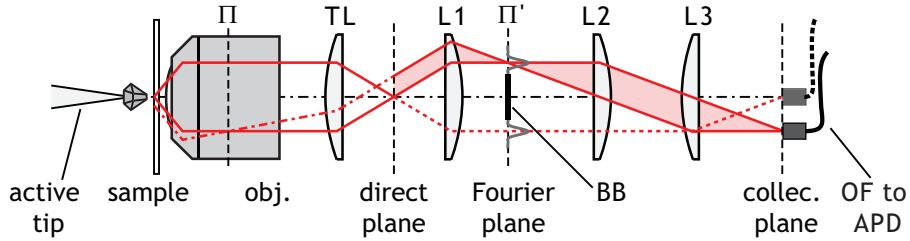


Fig. 1. Layout of the experimental setup: obj.= X100 oil immersion objective of effective numerical aperture $NA = 1.35$; TL= tube lens; L_1, L_2 (removable), L_3 = achromatic lenses; BB= beam block; OF= multimode optical fiber; APD= avalanche photodiode. Π' is the back-focal plane of L_1 . Π is the objective back-focal plane and is located inside the objective itself [5]. The OF-APD combination can be replaced by a camera (not sketched) aligned with the optical axis for imaging. In this setup, the tip is fixed and the sample is scanned in all three dimensions with nanometer accuracy. The remaining excitation at 515 nm is removed by an optical filter (not shown). A limited number of light rays are indicated for clarity.

correlation measurements [15-18]. This means that the quantum source cannot emit more than three to four photons at a time.

The diamond is illuminated with a $\lambda_{exc.} = 515$ nm laser light shone into the single mode optical fiber that is terminated by the tip. As we have shown previously [16-18], the red-orange near-field fluorescence of the NVs is able to launch SPPs into the gold film, whereas the green laser excitation cannot do that because of strong interband absorptions in gold in this wavelength range: this is a second motivation for using a nanodiamond tip. Finally, our arrangement generates a range of undesired cross-excited nonplasmonic lights such as gold fluorescence in addition to the useful plasmonic signal: this will be advantageously used to demonstrate the ability of our method to discriminate among useful and spurious signals. In the quantum regime, where only a few photons couple to SPPs, it is crucial to eliminate this spurious light.

Apart from the use of an active tip, our setup has additional special features. First, a removable Fourier lens L_2 is implemented. In the absence of L_2 , the light is collected in the direct space in a standard way. In this case, the collection fiber (OF in Fig. 1) is optimally placed along the optical axis and the collected signal is sent to the APD. Now adding L_2 so that the back-focal plane Π' of the microscope is conjugated with the collection plane allows collecting light in the Fourier space [5,16-18] (note that the Π' plane plays the same role as the back-focal plane of the objective Π that is located inside the objective itself and is difficult to access for optical imaging). In this case, the collection fiber OF can be laterally displaced to focus on the SPP useful signal only (see below), as shown schematically in Fig. 1. In addition, an optional beam block (BB in Fig. 1) of adjusted lateral extension can be added in the Fourier plane to remove all of the allowed light that couples into the silica substrate at smaller incidences not exceeding θ_C [18]. Finally, the collection fiber can be replaced by a wide-field camera to obtain either real-space or Fourier-space instantaneous images of the SPP propagation for a given tip position.

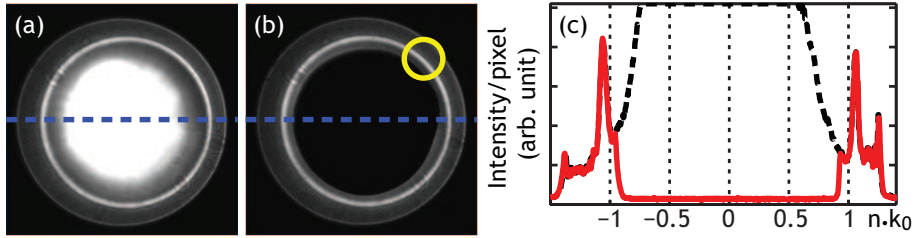


Fig. 2. a) Unfiltered and (b) filtered LRM images acquired in the Fourier plane. In (b), the small circle in the upper-right part of the SPP circle marks the imprint of the optical fiber OF used for image reconstruction. (c) Cross sections of (a) and (b) along the blue dashed lines.

3. Results and discussion

The principle of our method can be introduced by commenting on the Fourier-space LRM images shown in Figs. 2(a) and 2(b), which are obtained with the tip positioned in the near field of a 30-nm thick gold film. The Fourier lens L_2 is set in and the image is recorded on the camera. In order to filter the light emitted in the allowed-light cone we introduce a beam block (BB in Fig. 1) centered in the Fourier space (compare Figs. 2(a) and 2(b)). A distinctive bright circle can be seen in both images. It is typical for a SPP field generated at the air-gold interface and leaking into the silica substrate [2,5,16-20] at leakage radiation angles $\theta_{LR} > \theta_C$, as a consequence of phase matching at the gold-silica interface. Here θ_{LR} is spread over an angular 2° range ($\theta_{LR} \in [45^\circ, 47^\circ]$) because of the phonon broadening in the NV emission used for SPP excitation [21]. The SPP circle corresponds to an effective index $n_{SPP} \simeq 1.06 - 1.07 > 1$. It therefore falls in the forbidden-light zone and, as such, can only be detected with a $NA > 1$ objective. It represents a clear SPP signature, essentially cleaned from any spurious light, which couples in silica at smaller incidences up to θ_C [18] as already mentioned. Cross sections shown in Fig. 2(c) illustrate the importance of filtering the allowed light for clean SPP imaging. From unsaturated images (not shown) we estimate the fraction of spurious light to $\simeq 70\%$ of the total integrated signal in Fourier space. Therefore, in the following, we only focus our attention on those photons emitted in the forbidden-light region.

Our method consists of mapping the intensity of the SPP circle while the plasmonic system is raster scanning under the tip. For this purpose, the multimode fiber OF is positioned in the detection plane (Fig. 1) so as to coincide with this SPP circle. The small circle in the upper-

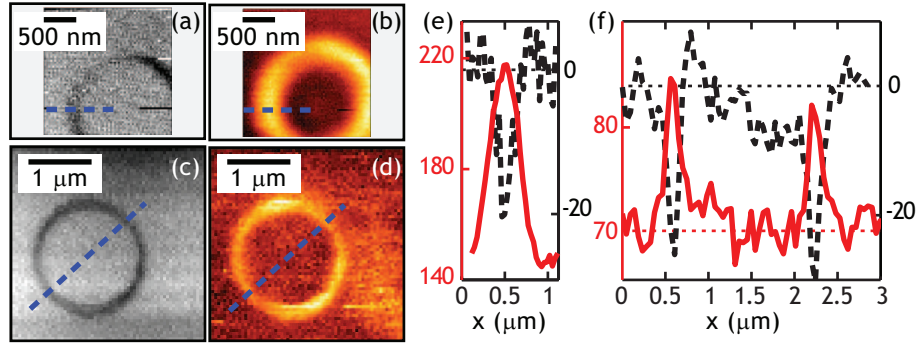


Fig. 3. Demonstration of the image reconstruction method. (a) and (c) Topographic images recorded simultaneously with the optical images (b) and (d), respectively. (b) Direct-space image obtained by scanning the slit under the nanodiamond tip. (d) Reconstructed image obtained by mapping the intensity of the SPP circle as function of the slit position under the tip. (e) [respectively (f)] Cross sections along the blue dashed lines in (a) and (b) [respectively (c) and (d)]. Left scales stand for the optical signal levels, expressed in units of kHz, right scales stand for the topography levels, expressed in nm.

right part of the SPP circle in Fig. 2(b) marks the imprint of OF used for image reconstruction. Note that only a small portion of the SPP circle will be mapped out. This does not affect the useful signal-to-background ratio since the spurious light is already filtered. To demonstrate our method, we have chosen to image a circular slit of $\simeq 120$ nm rim thickness and $\simeq 1.5$ μm inner diameter patterned by focused-ion beam (FIB) milling in a 30 nm thick gold film. The results are shown in Fig. 3. It is clear that the reconstructed image in Fig. 3(d) is much better resolved than the direct space image depicted in Fig. 3(b). As a matter of fact, the sharpness of the reconstructed image competes with that of the simultaneously acquired topographic image [22] in Fig. 3(c). This is confirmed by the cross sections shown in Figs. 3(e) and 3(f). In Fig. 3(f), the full width at half maximum of the optical signal is around 130 nm, to compare to 100 nm [23] in the corresponding topographic cross section, whereas in Fig. 3(e), it is as large as 230 nm, compared to 120 nm in the topography. Therefore, reconstructed images from the Fourier-filtered signals made only of high spatial frequencies, i.e. those due to SPPs leaking in the silica substrate, exhibit a four times enhanced spatial resolution of $\simeq 130 - 100 = 30$ nm compared to $\simeq 230 - 120 = 110$ nm obtained in the direct space. This clearly shows the advantage of our method concerning resolution. It is worthwhile to note that this 30 nm resolution fits well with the size of the nanodiamond and with the typical distance between tip and surface [22] during scanning. Therefore, our imaging method is close to reaching the optimal spatial resolution achievable with a point-like optical tip [14].

We now wish to give some insight into the physics governing our observations. We first point out that after Fourier filtering the recorded image represents a fair measure of the local amplitude of the excitation field at $\lambda = 515$ nm. More precisely, below the saturation regime of the NVs where we are working, the fluorescence signal $I(\mathbf{r})$ at the tip location \mathbf{r} is proportional to the excitation rate $R(\mathbf{r}) \propto |\boldsymbol{\mu} \cdot \mathbf{E}_{\text{exc.}}(\mathbf{r})|^2$ that depends on the local (incident+ reflected) field at the NV location ($\boldsymbol{\mu}$ is a transition dipole). R is strongly affected by the environment in the vicinity of the nanostructure [24, 25]. With our detection protocol only those emitted photons coupling directly to SPPs or scattered by the structure at $\theta \simeq \theta_{LR}$ are recorded and contribute to the signal shown in Fig. 3(d). The increased contrast between Figs. 3(b) and 3(d) suggests that the coupling of the incident light at θ_{LR} is enhanced only in the close vicinity of the aperture rim. This is also in qualitative agreement with recent works [6-18] showing that plasmonic cou-

plings depend critically on the distance between the quantum emitter and the nanostructure. We remark that, while the light emission with the tip located far away from the rim is dominated by the leaky SPP signal, the signal increase $\delta I/I \simeq 10\%$ observed in the close vicinity of the structure results from a competition between plasmonic and non plasmonic light (such as scattering and spurious fluorescence) emitted at $\theta \simeq \theta_{\text{LR}}$. Further analysis is required to identify the emission channel responsible for the increase in resolution reported in this work.

It is worth pointing out that in Refs. [2, 4], SPP imaging was obtained with a classical NSOM aperture-tip illuminated at a fixed laser wavelength. In particular, SPP fringes were observed while scanning the tip in the vicinity of local protrusions [2] or inside a square cavity made of grooves [4] (see also the theoretical analysis in Refs. [26, 27]). The absence of fringes in Fig. 3(d) is related to the fact that in our working regime we do not image the local photonic density-of-states at the emission wavelengths of the NV but the local excitation variation $R(\mathbf{r})$ at $\lambda_{\text{ex}} = 515$ nm. Since no SPP is excited at this wavelength no oscillation or fringe is expected to show up [24].

Before summarizing, it is worth commenting on an additional feature of our method. It was found recently that Fourier filtering can lead to strong image distortions in the direct space in such a way that the intense SPP signal expected at the center of the direct-space LRM images can be completely washed out [16, 17]. This is due to interferences arising between propagating SPP modes and the residual transmitted light (here the NV fluorescence) [28]. In the present work, we even found that it was not possible to image the circular rim in the direct space as shown in Fig. 3(b), but with the Fourier filter in place. This complication is avoided by working in the Fourier space. A similar conclusion was reached recently in experiments aimed at probing the second-order coherence of SPPs launched by quantum emitters into a metallic film [18]. Finally, it is worth recalling that high lateral resolution imaging was reported long time ago using the so called apertureless scanning plasmon near-field microscope (SPNM) based on scanning tunnelling microscopy (STM) methods [29]. It would be interesting to compare precisely our method with this SPNM approach, in particular in view of the recent development of STM methods coupled to LRM [30, 31].

4. Conclusion

In summary, by probing leaky SPPs launched by a scanning quantum Emitter, we have demonstrated a simple method to image a plasmonic device - a circular ring in a thin gold film - with a four times enhanced spatial resolution, i.e. a $\simeq 30$ nm resolution. The method implies working in the Fourier space to reconstruct images in the direct space from SPP signals that are cleaned from detrimental contributions with short spatial frequencies. We believe that the approach presented here will be of interest to applications in the emerging field of quantum plasmonics in general, and for local studies of quantum emitters coupled to metal films in particular [6, 25].

Acknowledgements: We thank G. Dantelle and T. Gacoin for providing us with nanodiamond samples and Jean-François Motte for the optical tip manufacturing and FIB milling. This work was supported by Agence Nationale de la Recherche (ANR), France, through the PLASTIPS and NAPHO projects.